

INITIAL VALUE TECHNIQUES FOR THE HELMHOLTZ AND MAXWELL EQUATIONS*

Frank Natterer and Olga Klyubina

(Department of Mathematics, University of Münster, Einsteinstrasse 62, 48149 Münster, Germany)

Email: nattere@math.uni-muenster.de, klyubina@math.uni-muenster.de

Abstract

We study the initial value problem of the Helmholtz equation with spatially variable wave number. We show that it can be stabilized by suppressing the evanescent waves. The stabilized Helmholtz equation can be solved numerically by a marching scheme combined with FFT. The resulting algorithm has complexity $n^2 \log n$ on a $n \times n$ grid. We demonstrate the efficacy of the method by numerical examples with caustics. For the Maxwell equation the same treatment is possible after reducing it to a second order system. We show how the method can be used for inverse problems arising in acoustic tomography and microwave imaging.

Mathematics subject classification: 35J05, 65N21.

Key words: Stability of elliptic initial value problems, Parabolic wave equation, Inverse problems in acoustics and electromagnetics.

1. Introduction

The initial value problem for elliptic equations, such as the Helmholtz and the Maxwell equations, are notoriously unstable. There exists a huge literature on stabilizing these initial value problems. Common features of these works are the use of a-priori information about the exact solution and conditional stability estimates; see [1]. For a recent paper that provides an overview and the spirit of these works see [2].

In this paper we follow a completely different route. We consider a differential equation of the form

$$\Delta u + k^2(1 + f(x))u = 0. \quad (1.1)$$

For a large parameter k we show that the Cauchy initial value problem for this equation is perfectly stable, provided we restrict ourselves to low frequencies, *i.e.*, the part of the solution u that is obtained by low-pass filtering u with a cut-off frequency near k . In other words, the instability is a pure high frequency phenomenon and disappears as soon as the high frequencies are removed. We do not need a-priori assumptions, and our estimates are linear. Physically our stabilization means the removal of the evanescent waves.

Estimates of this type were derived in [7] for the Helmholtz equation and in [6] for the Maxwell equations by energy estimates. These estimates contain powers of order 2 and even 4 of k which make the application to high frequency imaging questionable. In Section 2 we derive new estimates with a much better behavior in terms of k . In fact they have negative powers of k . These new estimates are based on the thesis [10]. They can be viewed as the analogue of the

* Received October 31, 2006; Final revised November 21, 2006.

famous $1/k$ estimates for the inverse Helmholtz operator of [4] and [3]; they are also reminiscent of the recent work [9]. In Section 3 we give numerical examples for initial value problems with a focal point. In Section 4 we demonstrate the usefulness of the initial value approach to inverse problems.

2. Stability Estimates

For simplicity we restrict ourselves to the Helmholtz case with zero initial values, *i.e.*, we consider the initial value problem

$$\Delta u + k^2(1 + f)u = r, \quad x_2 > 0, \quad u(x_1, 0) = 0, \quad \frac{\partial u}{\partial x_2}(x_1, 0) = 0. \tag{2.1}$$

Theorem 2.1. *Let $f \in C^1(\mathbb{R}^2)$ be real valued and supported in $[-\rho, \rho] \times [0, \infty]$, and let m be a constant such that $-1 < m \leq f$. Then, for $\kappa = \theta k \sqrt{1 + m}, 0 < \theta < 1$, there exists a constant c such that*

$$\|u_{k\vartheta}(\cdot, x_2)\|_{L_2(-\rho, \rho)} \leq \frac{\sqrt{\rho} e^{\rho c}}{k\vartheta} \|r\|_{L_2(-\rho, \rho) \times (0, \rho)}, \tag{2.2}$$

where

$$\vartheta = \sqrt{1 + m} \sqrt{1 - \theta^2}. \tag{2.3}$$

Proof. In a first step we assume f to be piecewise constant as a function of x_2 , *i.e.*,

$$f(x_1, x_2) = f_i(x_1), \quad ih \leq x_2 \leq (i + 1)h$$

with some $h > 0$. Fourier transforming (2.1) with respect to x_1 yields for $ih \leq x_2 \leq (i + 1)h$

$$\frac{d^2}{dx_2^2} \hat{u}(\cdot, x_2) + A_i \hat{u}(\cdot, x_2) = \hat{r}(\cdot, x_2), \tag{2.4}$$

the operator A_i in $L_2(\mathbb{R}^1)$ being defined by

$$(A_i v)(\xi_1) = (k^2 - \xi_1^2)v(\xi_1) + (2\pi)^{-1/2} k^2 (\hat{f}_i * v)(\xi_1)$$

with $*$ the convolution in \mathbb{R}^1 . Since f is real, A_i is selfadjoint. We have by Parseval's relation

$$\begin{aligned} (\hat{f}_i * v, v)_{L_2(\mathbb{R}^1)} &= \int_{-\infty}^{+\infty} (\hat{f}_i * v) \bar{v} d\xi_1 = \int_{-\infty}^{+\infty} \widetilde{(\hat{f}_i * v)} \bar{v} dx_1 \\ &= (2\pi)^{1/2} \int_{-\infty}^{+\infty} f_i |\tilde{v}|^2 dx_1 \geq (2\pi)^{1/2} m (v, v)_{L_2(\mathbb{R}^1)}. \end{aligned}$$

Applying this to functions v supported in $[-\kappa, \kappa]$ we obtain for the restriction of A_i to $L_2(-\kappa, \kappa)$ (again denoted by A_i)

$$(A_i v, v)_{L_2(-\kappa, \kappa)} \geq (k^2 - \kappa^2 + k^2 m)(v, v)_{L_2(-\kappa, \kappa)}.$$

Integrating (2.4) over $[ih, x_2]$ we obtain

$$\begin{aligned} \hat{u}(\cdot, x_2) &= \cos(K_i(x_2 - ih)) \hat{u}(\cdot, x_2) + K_i^{-1} \sin K_i(x_2 - ih) \frac{\partial \hat{u}}{\partial \xi_1}(\cdot, x_2) \\ &\quad + \int_{ih}^{x_2} K_i^{-1} \sin(K_i(x_2 - x'_2)) \hat{r}(\cdot, x'_2) dx'_2, \end{aligned} \tag{2.5}$$

where $K_i = \sqrt{A_i}$. For this to make sense we assume that A_i is positive definite, this being the case for $k^2 - \kappa^2 + k^2m > 0$, i.e., for $\kappa < k\sqrt{1+m}$. For $\kappa = \theta k\sqrt{1+m}$, $0 < \theta < 1$ the eigenvalues of K_i are $\geq k\sqrt{1+m}\sqrt{1-\theta^2} = k\vartheta$. For $|\xi_1| < \kappa$ we put

$$U_i(\xi_1) = \left(\hat{u}(\xi_1, ih), \frac{\partial \hat{u}}{\partial x_2}(\xi_1, ih) \right)^T.$$

From (2.5) we obtain

$$U_{i+1} = L_i U_i + \int_{ih}^{(i+1)h} J_i(x'_2) \hat{r}(\cdot, x'_2) dx'_2, \tag{2.6}$$

where

$$L_i = \begin{pmatrix} \cos(K_i h) & K_i^{-1} \sin(K_i h) \\ -K_i \sin(K_i h) & \cos(K_i h) \end{pmatrix}, \quad J_i(x'_2) = \begin{pmatrix} K_i^{-1} \sin(K_i((i+1)h - x'_2)) \\ \cos(K_i((i+1)h - x'_2)) \end{pmatrix}.$$

Solving the recursion (2.6) yields

$$U_i = L_{i-1} \cdots L_0 U_0 + \sum_{j=0}^{i-1} L_i \cdots L_{j+1} \int_{jh}^{(j+1)h} J_j(x'_2) \hat{r}(\xi_1, x_2) dx'_2.$$

Obviously $L_i = D_i Q_i D_i^{-1}$ with

$$Q_i = \begin{pmatrix} \cos(K_i h) & \sin(K_i h) \\ -\sin(K_i h) & \cos(K_i h) \end{pmatrix}, \quad D_i = \begin{pmatrix} I & 0 \\ 0 & K_i \end{pmatrix}.$$

With $\|\cdot\|$ the Euclidean norm we have

$$\|Q_i\| = 1, \quad \|D_i^{-1} D_{i-1}\| \leq 1 + ch,$$

where $c > 0$ is a constant. Hence

$$\begin{aligned} & L_i \cdots L_{j+1} J_j(x'_2) \\ &= \prod_{k=j+2}^i D_k Q_k D_k^{-1} D_{j+1} Q_{j+1} \begin{pmatrix} K_j^{-1} \sin(K_j(j+1)h - x'_2) \\ K_{j+1}^{-1} \cos(K_j((j+1)h - x'_2)) \end{pmatrix} = D_i M_{ij}, \end{aligned}$$

where

$$\|M_{ij}\| \leq \frac{(1 + ch)^{i-j+1}}{k\vartheta}.$$

Since $U_0 = 0$ we finally get

$$U_i = D_i \sum_{j=0}^{i-1} \int_{jh}^{(j+1)h} M_{ij}(x'_2) \hat{r}(jx'_2) dx'_2.$$

For the first component of U_i this implies

$$\begin{aligned} |\hat{u}(\xi_1, ih)| &\leq \frac{1}{k\vartheta} \sum_{j=0}^{i-1} (1+ch)^{i-j+1} \int_{jh}^{(j+1)h} |\hat{r}(\xi_1, x'_2)| dx'_2 \\ &\leq \frac{1}{k\vartheta} (1+ch)^i \int_0^{ih} |\hat{r}(\xi_1, x'_2)| dx'_2 \\ &\leq \frac{1}{k\vartheta} e^{cih} \sqrt{ih} \left(\int_0^{ih} |\hat{r}(\xi_1, x'_2)|^2 dx'_2 \right)^{1/2}. \end{aligned}$$

For $ih = x_2 \leq \rho$ it follows from $(1 + s/i)^i \leq e^s$ that

$$\begin{aligned} |\hat{u}(\xi_1, x_2)|^2 &\leq \frac{\rho e^{2\rho c}}{k^2 \vartheta^2} \int_0^\rho |\hat{r}(\xi_1, x'_2)| dx'_2, \\ \|u_{k\vartheta}(\cdot, x_2)\|_{L_2(-\rho, \rho)}^2 &\leq \frac{\rho e^{2\rho c}}{k^2 \vartheta^2} \|r\|_{L_2([- \rho, \rho] \times [0, \rho])}^2. \end{aligned}$$

So far we have dealt with the piecewise constant case. In order to get the general case we only have to let h tend to 0. This finishes the proof of Theorem 2.1.

Theorem 2.1 is a simplified version of a result of [10]. It is especially useful for large values of k . In fact it has been used in [10] for high frequency estimates for the geometric optics approximation to the inverse Helmholtz problem.

3. Numerical Example

It is easy to derive a numerical method from Theorem 2.1: We simply discretize (2.1) on a cartesian grid, march it in the x_2 direction, and apply a low pass filter in the x_1 direction with cut-off $k\vartheta$ after each marching step. From Theorem 2.1 we expect this procedure to be stable, and numerical evidence shows that this is in fact the case. The resulting algorithm needs $n^2 \log n$ on a $n \times n$ grid. This is only slightly more than for the algorithms that are based on the one way wave equation [5].

As an example we treat the scattering of a plane wave by the Luneberg lense

$$f(x) = 1 - 4|x|^2 \tag{3.1}$$

in the ball of radius 1/2 and $f = 0$ outside. It is well known that under plane wave insonification the Luneberg lens generates a focal point at its rim [11]. Due to this focal point we consider the Luneberg lens as a challenging test problem for a Helmholtz solver at high frequency. We are seeking a solution u of (1.1) that is of the form

$$u = e^{ikx_2} + u_s, \tag{3.2}$$

where the scattered field u_s satisfies the Sommerfeld radiation condition.

For our numerical experiment we used the wave number $k = 100$ and the cut-off frequency $\kappa = 90$. The computations are done in a square of side length 1. Real part and imaginary part

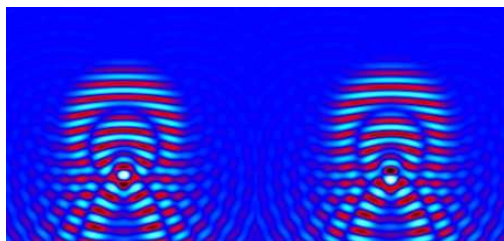


Fig. 3.1. Scattered field of Luneberg lens with plane wave illumination (plane wave coming in from top). Real part (left) and imaginary part (right).

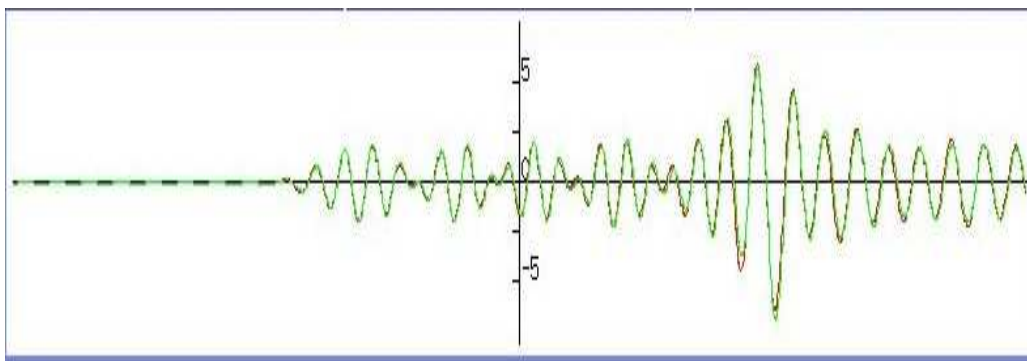


Fig. 3.2. Central vertical cross sections through real part of exact and approximate fields.

of the scattered field are displayed in Fig. 3.1. The focal point is clearly visible. The field was computed by a time domain finite difference method, followed by a Fourier transform.

In Fig. 3.2 we display central vertical cross sections through the real part of the exact field and of the approximate scattered field computed by the initial value technique, the Cauchy initial values being stipulated at the top boundary of the reconstruction region. We see that the agreement of exact and approximate fields is almost perfect.

4. Application to Inverse Problems

Since we need Cauchy initial values, i.e., values for u as well as for $\frac{\partial u}{\partial x_2}$ on the initial manifold, initial value techniques can't be used for the direct boundary value problem. However, in inverse problems, u is measured on the boundary of the reconstruction region, while $\frac{\partial u}{\partial x_2}$ is obtained by the Dirichlet-to-Neumann-map. Thus, Cauchy initial values are available, and initial value techniques can be used for the forward and for the adjoint problems. This applies also to the Maxwell equations

$$\operatorname{curl} E - ikH = 0, \quad \operatorname{curl} H + ik(1 + f)E = 0, \quad (4.1)$$

where we have written $n = 1 + f$ for the refractive index. We employ the usual procedure for eliminating H : With $\operatorname{div}(nE) = 0$ we obtain for E the second order equation

$$\Delta E - \nabla \operatorname{div} E + k^2(1 + f)E = 0. \quad (4.2)$$

This equation can be treated exactly as the Helmholtz equation; see [6].

The application of the initial value technique to the inverse problems of the Helmholtz and Maxwell equation (usually referred to as inverse scattering problems) is as follows. For iterative methods, the differential equation and its adjoint have to be solved repeatedly, often hundreds of times. Both computations can be done efficiently by the initial value techniques described above. The use of initial value techniques is in fact quite common in inverse scattering. Methods competing with our initial value technique are the various forms of one-way wave equations and the paraxial or parabolic approximation to the wave equation [5]. The advantage of our approach is its simplicity and its ability to handle backscatter. Numerical results for Helmholtz and Maxwell equations are presented in [6, 7].

References

- [1] F. John, Continuous dependence on data for solutions of partial differential equations with a prescribed bound, *Commun. Pure Appl. Math.*, **13** (1960), 551-587.
- [2] L. Elden and F. Berntsson, Stability estimates for a Cauchy problem for an elliptic partial differential equation, *Inverse Probl.*, **21** (2005), 1643-1653.
- [3] N. Burq, Semi-classical estimates for the resolvent in non-trapping geometries, *Int. Math. Res. Notes*, **5** (2002), 221-241.
- [4] S. Agmon, Spectral properties of Schrödinger operators and scattering theory, *Annali della Scuola Norm. Sup. die Pisa*, **11** (1975), 151 - 218.
- [5] M.D. Collins and W.L. Siegmann, *Parabolic Wave Equations with Applications*, Springer, 2001.
- [6] M. Vögeler, Reconstruction of the three-dimensional refraction index in electromagnetic scattering by using a propagation-backpropagation method, *Inverse Probl.*, **19** (2003), 739-754.
- [7] F. Natterer and F. Wübbeling, Marching schemes for inverse acoustic scattering problems, *Numer. Math.*, **100** (2005), 697-710.
- [8] F. Natterer, An initial value approach to the inverse Helmholtz problem at fixed frequency, in *Inverse Problems in Medical Imaging and Nondestructive Testing*, H.W. Engl, A.K. Louis and W. Rundell (Eds.), Springer, 1997.
- [9] V. Isakov and T. Hrycak, Increased stability in the continuation of solutions to the Helmholtz equation, *Inverse Probl.*, **20** (2004), 697-712.
- [10] O.V. Klyubina, *Asymptotic methods in ultrasound tomography*, Thesis, Department of Mathematics and Computer Science, University of Münster, 2005.
- [11] S.P. Morgan, General solution of the Luneberg lens problem, *J. Appl. Phys.*, **29** (1958), 1358-1368.